IUST
Iran University of Science and Technology

Iranian Journal of Electrical and Electronic Engineering

Journal Homepage: ijeee.iust.ac.ir

Analysis of Partial Discharge Measurements using Coupling Capacitor in Rotating Machine

Ahmad Syukri Abd Rahman*, Mohamad Nur Khairul Hafizi Rohani**(C.A.), Nur Dini Athirah Gazata**, Afifah Shuhada Rosmi**, Ayob Nazmi Nanyan**, Aiman Ismail Mohamed Jamil**, Mohd Helmy Halim Abdul Majid*, Normiza Masturina Samsuddin*

Abstract: Partial discharge (PD) is a significant concern in the operation of rotating machines such as generators and motors, as it can lead to insulation degradation over time, reducing the reliability and lifespan of the machines. To monitor PD activity, coupling capacitors (CC) are widely used as sensors for online PD detection, as they can effectively capture PD pulses in high-voltage (HV) rotating machines. The primary objective of this research is to measure and analyze PD signals using a CC sensor for HV rotating machines under varying input voltages and frequencies, following the guidelines of the IEC 60270 standard and utilizing the MPD 600 device. The experimental setup includes performing insulation resistance (IR) testing, PD calibration, and PD measurement. Additionally, this paper provides a detailed study of PD signal characteristics, specifically focusing on phase-resolved partial discharge (PRPD) patterns, to understand the behavior of PD in HV rotating machines, enhancing fault diagnosis and preventive maintenance strategies.

Keywords: Partial Discharge (PD); Coupling Capacitor (CC); High Voltage Rotating Machine (HVRM); Phase Resolve Partial Discharge (PRPD).

1 Introduction

PARTIAL discharge (PD) monitoring in rotating machines represents a critical challenge in power system reliability and maintenance. These discharges, while individually small, can progressively degrade insulation systems and lead to catastrophic failures if left undetected. The economic impact of such failures in industrial settings can be substantial, involving both replacement costs and operational downtime.

Previous research has made significant contributions to PD detection methods. Stone et al. [1] demonstrated that conventional PD measurement techniques, while functional, often struggle with noise discrimination in industrial environments. Chai et al. [4] explored UHF sensors for PD detection, establishing their effectiveness in power system equipment but noting limitations in rotating machine applications. Yamanaka et al. [7] investigated corona discharge effects on rotating machine insulation, highlighting the need for more precise detection methods.

Despite these advances, several crucial challenges remain unresolved. These include the difficulty in distinguishing between genuine PD signals and background noise in industrial environments, limited sensitivity and reliability of existing measurement techniques in high-voltage applications, cost-effectiveness concerns in implementing PD monitoring

Iranian Journal of Electrical & Electronic Engineering, 2025.
Paper first received 31 Dec 2024 and accepted 06 Mar 2025.
* The author is with the MHH Condition Monitoring Sdn Bhd, No.8, Tingkat 1, Jalan Sumazau 1J/KU5, Bandar Bukit Raja, 41050 Klang, Selangor, Malaysia.
E-mails: ahmadsyukri@studentmail.unimap.edu.my, helmy.uitm@mhhlegacy.com.my, normiza@mhhlegacy.com.my
** The author is with the Faculty of Electrical Engineering & Technology, Universiti Malaysia Perlis (UniMAP), 02600 Arau, Perlis, Malaysia.
E-mails: khairulhafizi@unimap.edu.my, diniathirah@studentmail.unimap.edu.my, afifahshuhada@unimap.edu.my, ayobnazmy@unimap.edu.my, aimanismail@studentmail.unimap.edu.my
Corresponding Author: Mohamad Nur Khairul Hafizi Rohani

systems, and the need for standardized measurement protocols following IEC 60270 guidelines.

Our research addresses these gaps by introducing a comprehensive analysis of PD measurements using coupling capacitors (CC) in rotating machines. Unlike previous studies, we implement a systematic approach combining insulation resistance testing, PD calibration, and measurement. We analyze PD characteristics across varying input voltages and frequencies, with a specific focus on phase-resolved partial discharge (PRPD) patterns for enhanced fault diagnosis.

This study makes several key contributions to the field. First, it establishes a more reliable method for PD detection in rotating machines. Second, it provides detailed analysis of PD characteristics under various operating conditions. Third, it develops improved guidelines for implementing CC-based PD monitoring systems. Finally, it enhances understanding of PRPD pattern interpretation for maintenance decisions.

The remainder of this paper is organized as follows: Section 2 details our experimental methodology, including setup procedures and measurement protocols. Section 3 presents our results and analysis, focusing on PRPD pattern interpretation across different operating conditions. Section 4 discusses the implications of our findings and their practical applications in predictive maintenance strategies. Finally, Section 5 concludes with recommendations for future research directions.

2 Methodology

The PD testing was conducted at MHH Condition Monitoring Sdn. Bhd., Selangor, Malaysia. Three steps were involved to set up PD measurement such as IR test, PD calibration and PD measurement.

The first procedure is the Insulation Resistance (IR) test which is an essential measurement to evaluate the insulation system of rotating machine. The initial step is conducting an IR test is a key approach for determining the electrical insulation of 6 kV rotating machine which is crucial for detecting any faults like short circuit and breakdown before performing PD test [15]. Moreover, this to avoid damage to the equipment so that the equipment can be used to carry out PD testing while maintaining overall system reliability and safety [16]. Regular IR measurements allow for early detection of potential problems such as moisture ingress and insulation deterioration, enabling timely preventive maintenance interventions to prevent further deterioration. For safety reasons, it is essential to maintain sufficient IR to avoid electrical risks and failures [17].

There are several steps to run IR test where the first step begins with performing an IR test by de-energizing the equipment to ensure the safety of the testing process. Subsequently, the second step is to disconnect the equipment from the power source where the source was separated from terminal to off online PD. The third step is attached IR tester also called megger to check IR of the rotating motor. This can be identified by measuring the current flowing through the insulation. The red wire attaches to the winding and the black wire attaches to the ground. The IR test conducted between phase to ground that measures each insulation of the phase and the ground. Then, the forth step, 2.5 kV of DC voltage was injected to the winding of the motor for a set period. The measured IR is a key indicator of the effectiveness of insulation in preventing leakage currents.

The fifth step is to compare the IR values obtained with industry standards or equipment specifications to see if the measured insulation meets the required criteria which is above 100 MΩ. Finally, the sixth step is to record the measurement results, which include the recorded insulating resistance values as well as any significant observations. Hence, IR testing helps identify potential issues early on, allowing for smooth testing of PD. Fig. 1 shows the insulation resistance testing.

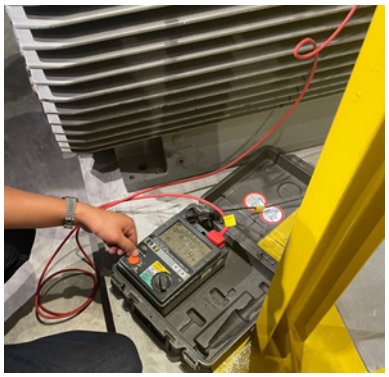

Fig 1. Insulation resistance testing

Next, Calibration of PD is an essential procedure for guaranteeing the dependability and security of electrical apparatus especially in HV rotating machine. PD calibration is an important process that aims to ensure the accuracy of measurements in PD activity in insulation of rotating machine [18], [19]. Lack of calibration may result inaccurate measurement that capture the charge associated with PD activity led to inaccurate results. Furthermore, PD calibration is necessary to determine divider factor (DF). The DF is an essential component in PD testing that helps scale and measure the PD signals precisely. The initial stage of PD calibration is assembling the required tools such as a voltage source CPC 100, PD calibration device CAL 542 which is known as charge calibration and CC.

The second step is to inject 1 kV voltage to the insulation system being tested after the setup is complete. The PD calibration CAL 542 has been set to 1 nC. The simulation OMICRON software for MPD 600

was open on PC, the frequency centre (fc) is set for 200 kHz while frequency bandwidth (Δf) is set for 300 kHz. At calibration settings, QIEC (target) was set to 1 nC. After that, press compute to determine DF value. The determination of the DF value occurs when the QIEC (measured) must be equal to or approximately 1 nC. Thereafter, the DF for different frequency center (fc) such as 0.2 MHz, 0.5 MHz, 2 MHz, 6 MHz, 10 MHz, 12 MHz, 14 MHz, 16 MHz, 18 MHz, and 20 MHz must be determined. Then, the data of DF was recorded to use as reference DF during PD measurement. This is to compare the detected PD signals with a reference standard to confirm measurement accuracy and reliability. Fig. 2 shows PD calibration set-up to ensure the accuracy of measurements in PD activity in insulation of rotating machine.

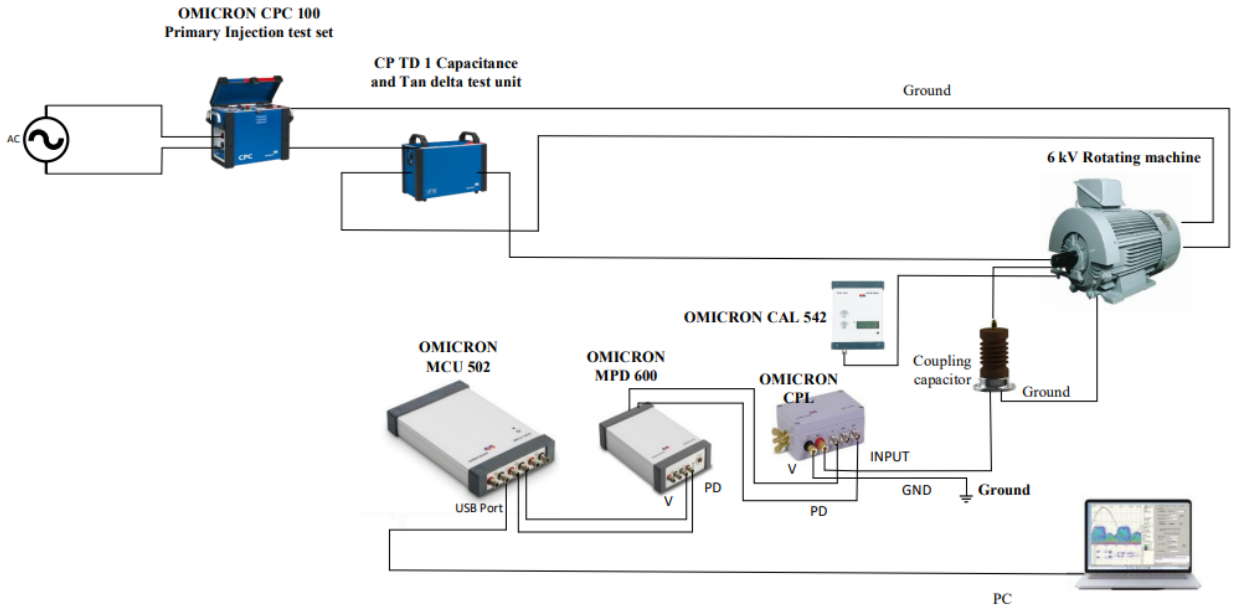

Fig 2. PD Calibration set-up

Lastly, the PD experimental setup is initiated by using the comprehensive test set OMICRON CPC 100 that includes the OMICRON CP TD booster. The OMICRON CPC 100 is the primary injection test set as main voltage source in charge of supplying power to the motor winding according to Figure 3. The CPC 100 is known for its versatility in electrical testing that is employed to ensure a comprehensive and controlled testing environment. The advantages of employing the CPC 100 lie in its capability to inject both voltage and current across a range of frequencies.

Next, the CP TD booster known as Capacitance/Dissipation Factor Testing Device is essential to the PD experimental setup. Mainly, its main objective is to make it easier to verify the insulation integrity of transformers, generators, and other HV system components in accordance with IEEE standards. One of this CP TD unique features is its capacity to run tests at different frequency bandwidth which helps identify possible signs of ageing in the insulation. The CP TD booster is an essential component that enhances and controls the voltage applied to the motor winding, hence improving the accuracy and dependability of the experimental configuration.

The CPC 100 connects to CP TD booster to inject different voltage 1 kV until 4 kV using different frequency bandwidth. By combining these parts, a steady and regulated power source is used to start the PD testing procedure which paves the way for precise and methodical evaluations of PD in the motor winding.

Then, the process begins by attaching the CC to the red phase of the motor establishing a connection from CC to the OMICRON CPL 542. The OMICRON CPL 542 known as external quadrupoles that connected MPD 600 PD measurement device which produce a reactive current that is greater than the capacity current of MPD 600 measurement device. Subsequently, the CPL 542 output connector's port is linked to the Multi-function Partial Discharge 600 (MPD 600). MPD 600 is high measurement accuracy for measuring PD activity.

The data transmitted from the MPD 600 port is then directed into the multi-device control unit 502 (MCU 502). The MCU is fiber optic bus controller that transforms optical signals into the common USB electrical communication signal. The optical signals are produced by the PD measurement device and sent to the MCU 502 control unit via fiber optic cables. The USB cable that is provided is used to connect the MCU 502 control device to the PC.

Finally, the PRPD pattern is analyzed using the OMICRON software after the PD measurement is finished. This specialized software is efficient for analyzing and interpreting the recorded PRPD patterns in depth. With its powerful capabilities, the OMICRON software allows for a thorough analysis of the discharge characteristics at various phases, which facilitates the identification of any issues or irregularities in the system being observed.

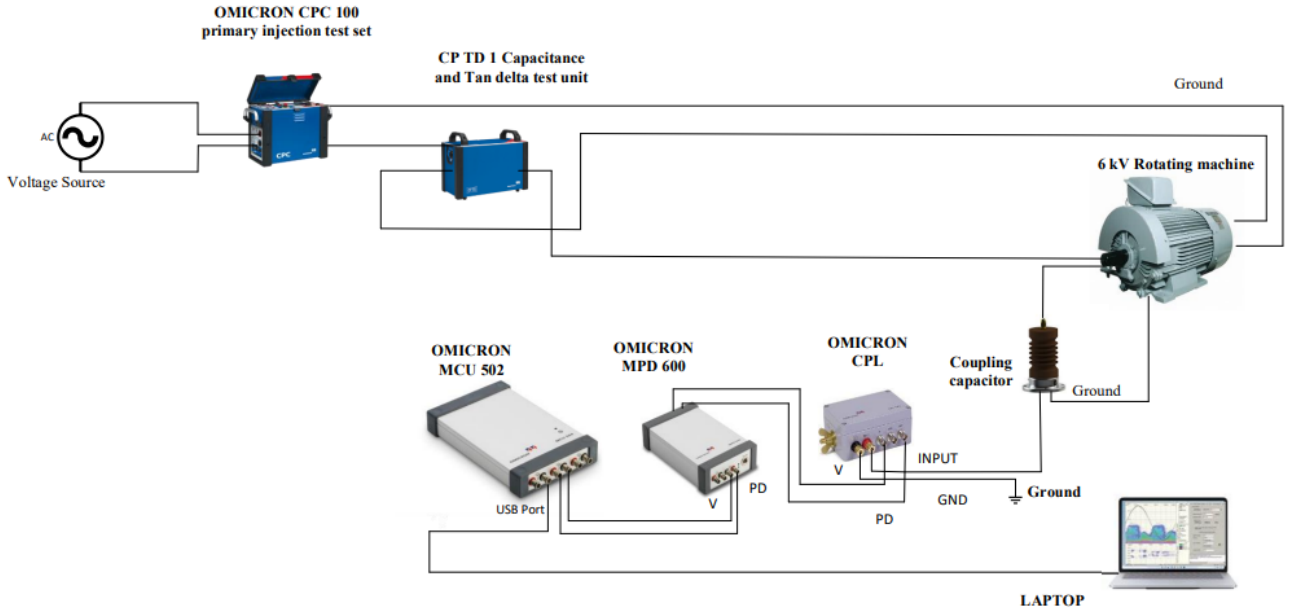

Fig 3. PD experimental set-up at MHH Condition Monitoring Sdn. Bhd.

3 Results and Discussion

3.1 IR Test Results

Table 1 presents IR test results for three phase windings of rotating machine that has been conducted. The results show red phase is 1.1 GΩ, yellow phase is 1.775 kΩ and blue phase is 900 MΩ. Table 1 interprets the red phase has higher resistance value which is 1.1 GΩ compared to the other phases. The higher the value indicating robust and good insulation. Due to that good insulation involves possessing a significant resistance to electrical current and the capability to sustain this high resistance consistently over an extended period.

On the other hand, a reading of yellow phase which is 1.1775 kΩ indicates a significantly lower IR. This could lead to poor insulation because of a resistance value that is comparatively low. The aging of IR is one factor that can result in low IR, thereby reducing its effectiveness in providing insulation. Lastly, a reading of 900 MΩ reflects an excellent level of IR. This high of a reading is ideal because maintaining the integrity of the insulation is crucial. Therefore, this indicates that the insulation is successfully preventing the flow of electric current.

In summary, only two-phase winding which are red and blue phase shows good IR. The IR must be above 100 MΩ as per IEC standard. Strong insulation that has a high resistance to current reduces the possibility of electrical problems like leakage currents or short circuits, which can cause electric shocks, fire hazards, or malfunctioning equipment. Interpreting these readings involves considering the specific requirements of the electrical system, the voltage involved, and industry standards to determine whether the insulation is within acceptable limits or if further actions, such as maintenance or replacement, are warranted.

Table 1. Insulation Resistance Result

Voltage (V)	Phase	Resistance (Ω)
2500	Red phase	1.1 GΩ
	Yellow phase	1.775 kΩ
	Blue phase	900 MΩ

3.2 PD Calibration Results

The results of the PD calibration at different frequency bands from 0.2 MHz to 20 MHz according to Table 2 provide important information about how the DF is affected. The DF, which represents the relationship between the signal output and the actual PD size, is an important parameter for accurately evaluating PD activity. Divider factor is a multiplier applied to the measured charge at the sensor during calibration. It compensates for energy loss caused by stray capacitance in the system, which can affect measurement accuracy [10]. The calibration process involves systematically evaluating the performance of the measurement system over different frequencies.

Furthermore, understanding the DF changes as the frequency rises from 0.2 MHz to 20 MHz is crucial to comprehending how the system reacts to various PD signals. Examining the calibration data can provide a comprehensive understanding of behavior of the system at different frequencies. This understanding can then be used to optimize and refine measurement parameters for accurate PD detection and assessment over a wide frequency range.

Table 2. Frequency centre and Divider Factor

Frequency Center (MHz)	Divider Factor (DF)
0.20	6.545
0.50	4.266
2.00	4.266
6.00	2.529
10.00	2.682
12.00	38.97
14.00	114.1
16.00	46.1
18.00	198.8
20.00	213.6

3.3 PD Measurements Results

This section discusses the findings of PD measurements made on the 6 kV motor at different frequencies both with and without micro voids activity. Ten selections of frequency bandwidth with different inject voltage were made for the measurements. Table 3 present the parameter of the PRPD pattern analysis using different frequency bandwidth at 1 kV injection voltage.

Table 3. PRPD parameter at 1 kV

F_{centre} (MHz)	Q_{IEC}/Q WTD (nC)	Q_{PEAK} (nC)	Q_{AVG} (nC)	n (kPDs/s)	PDis (mW)	DF
0.20	1.9520	2.6090	10.22	61.80	175.0	6.545
0.50	0.7583	0.9741	3.411	309.9	188.7	4.266
2.00	0.2279	0.2705	3.441	311.2	191.8	4.266
6.00	0.0217	0.0324	0.798	297.3	8.621	2.529
10.00	0.0089	0.0106	0.0615	298.0	3.968	2.682
12.00	0.3693	0.4433	0.4428	285.7	63.40	38.97
14.00	1.3400	1.5930	1.349	280.2	197.1	114.1
16.00	0.1141	0.1487	0.7573	275.9	57.86	46.1
18.00	0.2285	0.2594	0.761	296.2	258.2	198.8
20.00	0.0651	0.0769	0.6814	297.2	240.2	213.6

Fig. 4 shows there is no discharge on PRPD pattern, only disturbance from the rotating machine. This is because the sole occurrence of disturbance in the PRPD pattern could be attributed to either noise or interference within the measurement setup. This may be caused by noise interference or poor grounding during experimental set-up that led to effect accuracy of PD activity.

In some instances, low PD activity within the rotating machine may be indicated by the lack of the discharge of PRPD pattern. This is because low supplied voltage which 1 kV may be insufficient to create PD activity. PD is more noticeable when HV due to electrical stress on the insulating system is not high enough to start PD activity during low voltage.

PD activity is typically associated with HV that places greater stress on insulating materials. The electrical stress at 1 kV may be less than what is necessary for PDs to manifest or be detectable. In these situations, PD detection can be difficult and PD activity can be minimal due to the relatively low machine voltage levels. Apart from that, only small discharge occurred according to Fig. 4 (b), (e), (f) and (g). Fig. 4 shows Partial Discharge Inception Voltage (PDIV) which is the lowest voltage in an insulating system at which PD begins to happen. It is the voltage threshold at which PD activity starts and the insulating material starts to degrade.

Table 4 represents a parameter of the PRPD pattern analysis using different frequency bandwidth at 2 kV injection voltage.

Table 4. PRPD parameter at 2 kV

F_{centre} (MHz)	Q_{IEC}/Q WTD (nC)	Q_{PEAK} (nC)	Q_{AVG} (nC)	n (kPDs/s)	PDis (mW)	DF
0.20	1.045	3.865	1.005	58.00	9.324	6.545
0.50	0.7473	1.418	0.7726	229.5	39.51	4.266
2.00	0.2031	0.2682	0.2158	204.5	22.89	4.266
6.00	0.0226	0.0345	0.0229	274.9	3.094	2.529
10.00	0.0092	0.0109	0.0094	248.7	1.210	2.682
12.00	0.3513	0.4135	0.3485	217.8	25.05	38.97
14.00	1.4310	1.7120	1.429	212.3	74.41	114.1
16.00	0.1108	0.1399	0.1111	259.9	12.41	46.1
18.00	0.2276	0.2568	0.2281	275.6	17.99	198.8
20.00	0.0597	0.0715	0.0588	279.1	8.848	213.6

Fig. 5 (a) (e) shows there is discharge that appeared on PRPD pattern. According to Fig. 5 (a), the PRPD pattern clearly shows there is micro void discharge in rotating machine at 0.2 MHz. Fig. 5 (f) and (g) shows there is

discharge present on PRPD pattern at 12 MHz and 14 MHz.

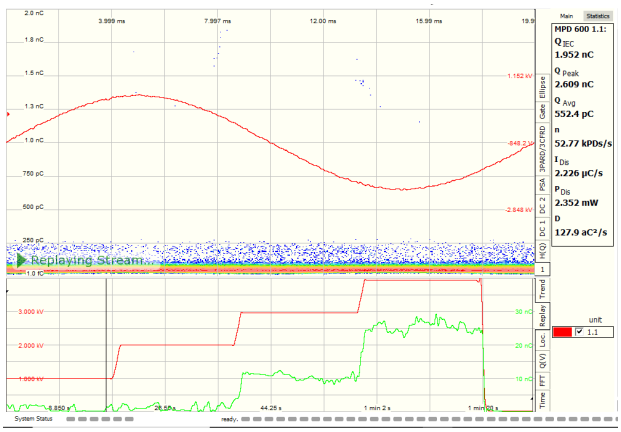

(a)

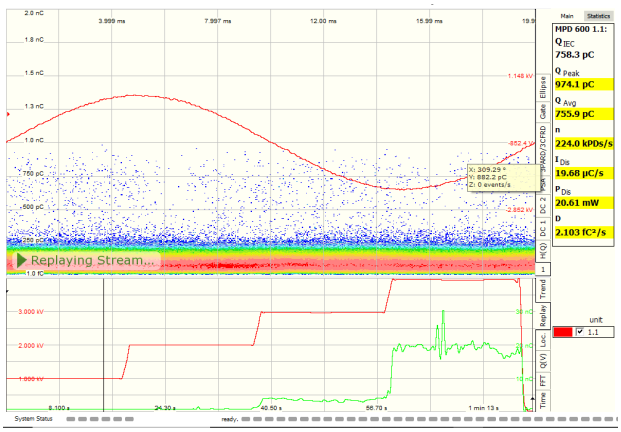

(b)

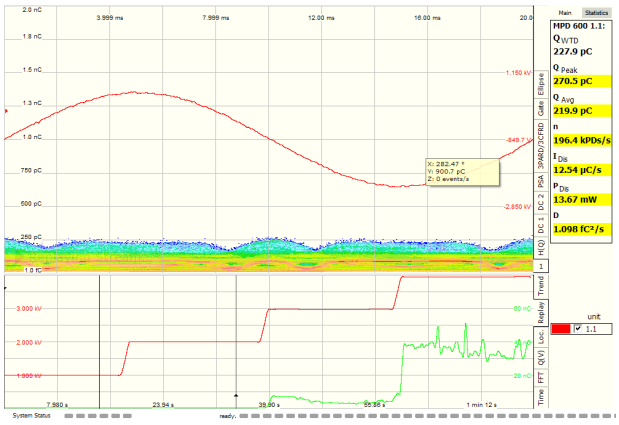

(c)

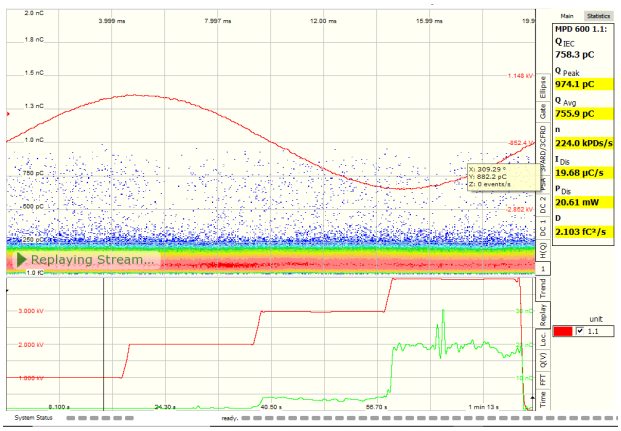

(d)

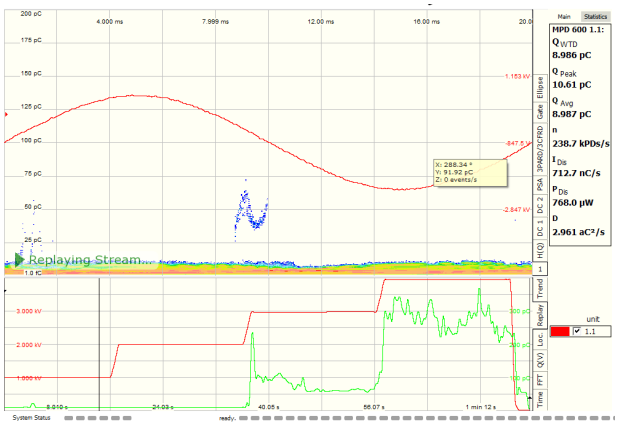

(e)

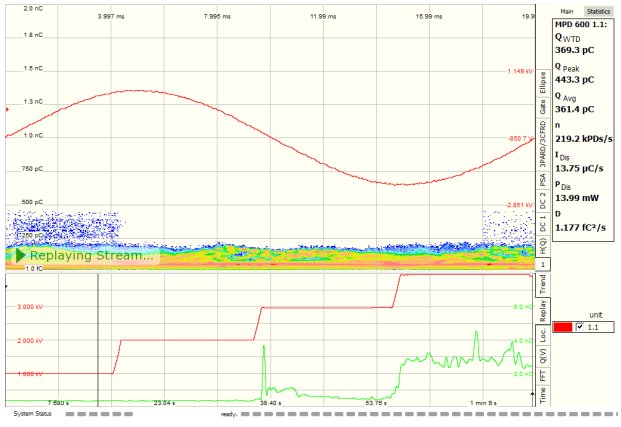

(f)

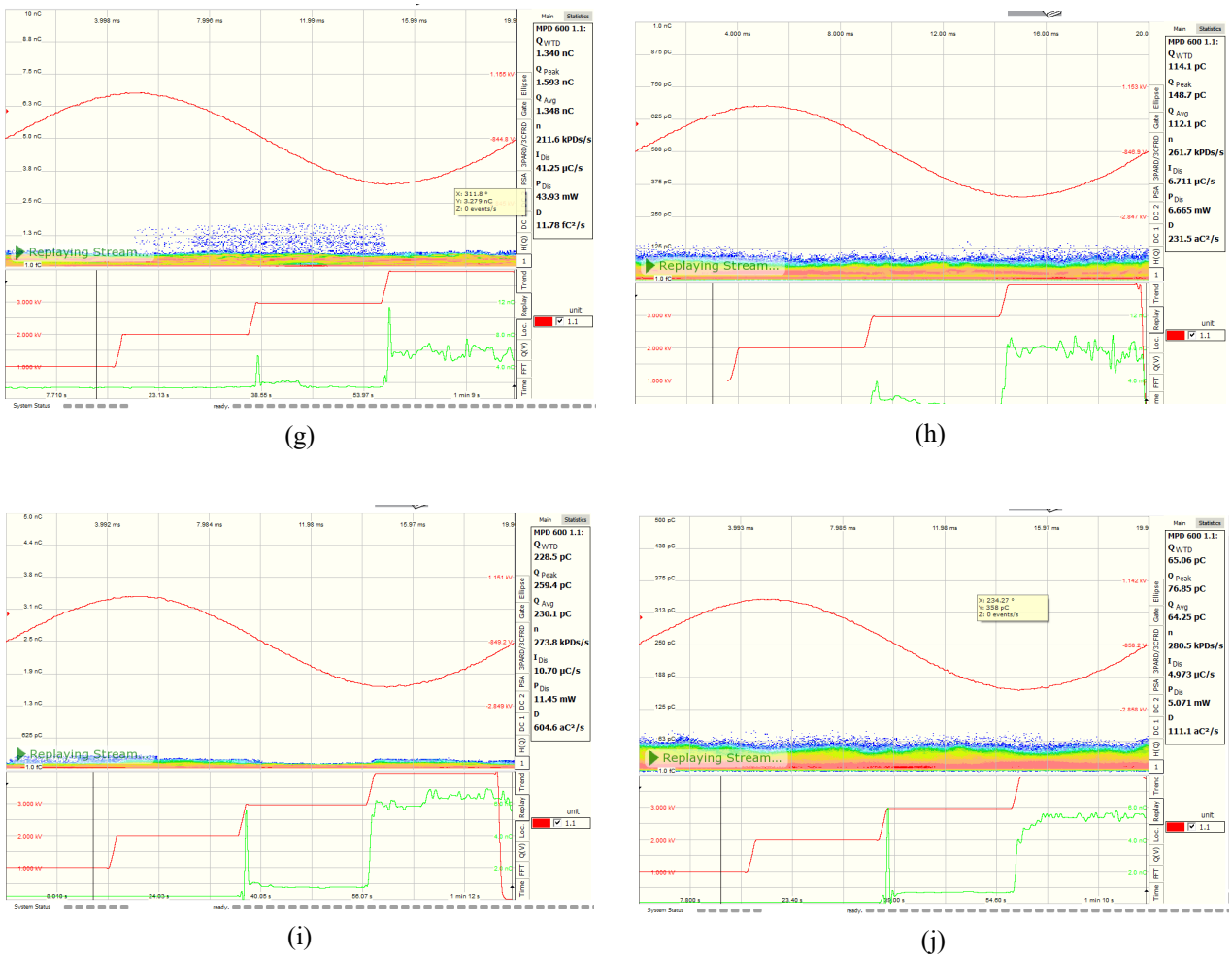

Fig 4. PRPD pattern for 1 kV (a) 0.2 MHz, (b) 0.5 MHz, (c) 2 MHz, (d) 6 MHz (e) 10 MHz (f) 12 MHz, (g) 14 MHz, (h) 16 MHz, (i) 18 MHz and (j) 20 MHz.

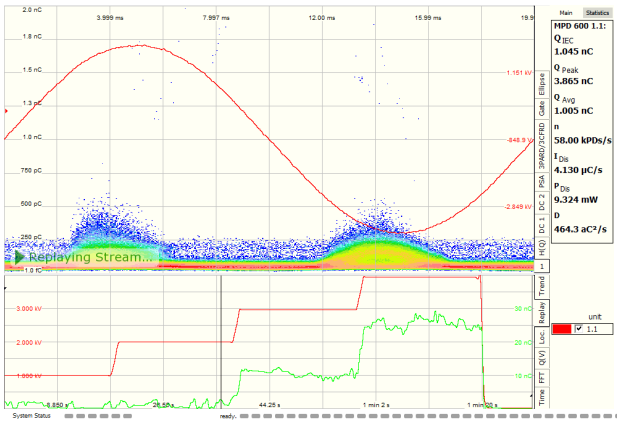
MPD 600 1.1:
Q IEC
1.045 nC
Q Peak
3.865 nC
Q Avg
1.005 nC
n
58.00 kPDs/s
I Dis
4.130 µC/s
P Dis
9.324 mW
D
464.3 aC²/s
Replaying Stream...

(a)

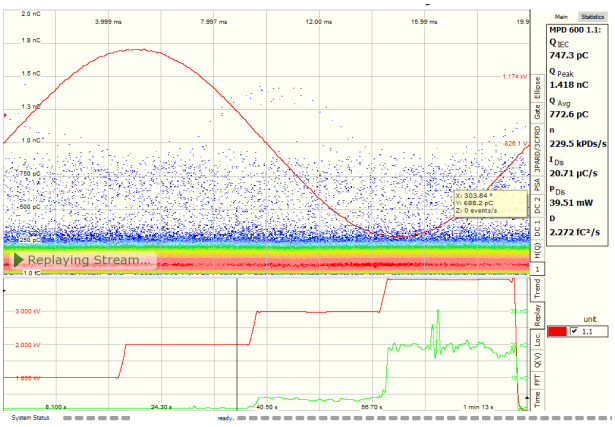
MPD 600 1.1:
Q IEC
747.3 pC
Q Peak
1.418 nC
Q Avg
772.6 pC
n
229.5 kPDs/s
I Dis
20.71 µC/s
P Dis
39.51 mW
D
2.272 fC²/s
Replaying Stream...

(b)

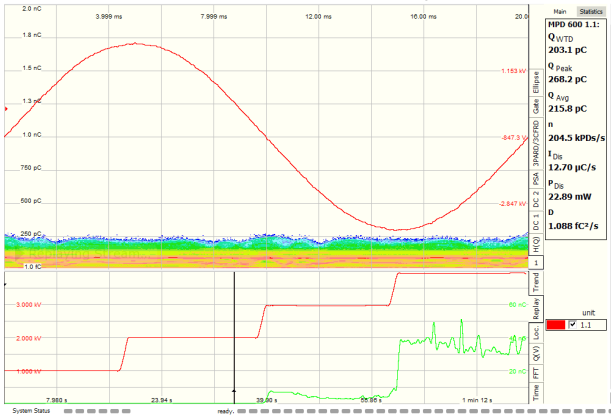
MPD 600 1.1:
Q WTD
203.1 pC
Q Peak
268.2 pC
Q Avg
215.8 pC
n
204.5 kPDs/s
I Dis
12.70 µC/s
P Dis
22.89 mW
D
1.088 fC²/s

(c)

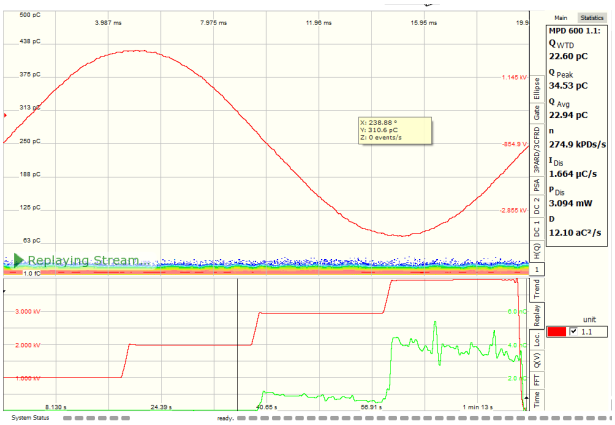
MPD 600 1.1:
Q WTD
22.60 pC
Q Peak
34.53 pC
Q Avg
22.94 pC
n
274.9 kPDs/s
I Dis
1.664 µC/s
P Dis
3.094 mW
D
12.10 aC²/s
Replaying Stream...

(d)

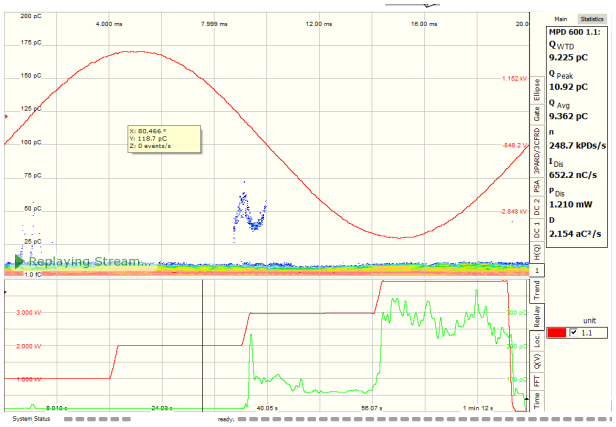
MPD 600 1.1:
Q WTD
9.225 pC
Q Peak
10.92 pC
Q Avg
9.362 pC
n
248.7 kPDs/s
I Dis
652.2 nC/s
P Dis
1.210 mW
D
2.154 aC²/s
Replaying Stream...

(e)

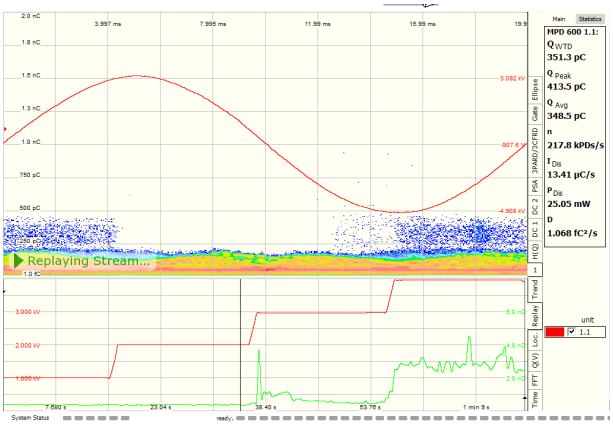
MPD 600 1.1:
Q WTD
351.3 pC
Q Peak
413.5 pC
Q Avg
348.5 pC
n
217.8 kPDs/s
I Dis
13.41 µC/s
P Dis
25.05 mW
D
1.068 fC²/s
Replaying Stream...

(f)

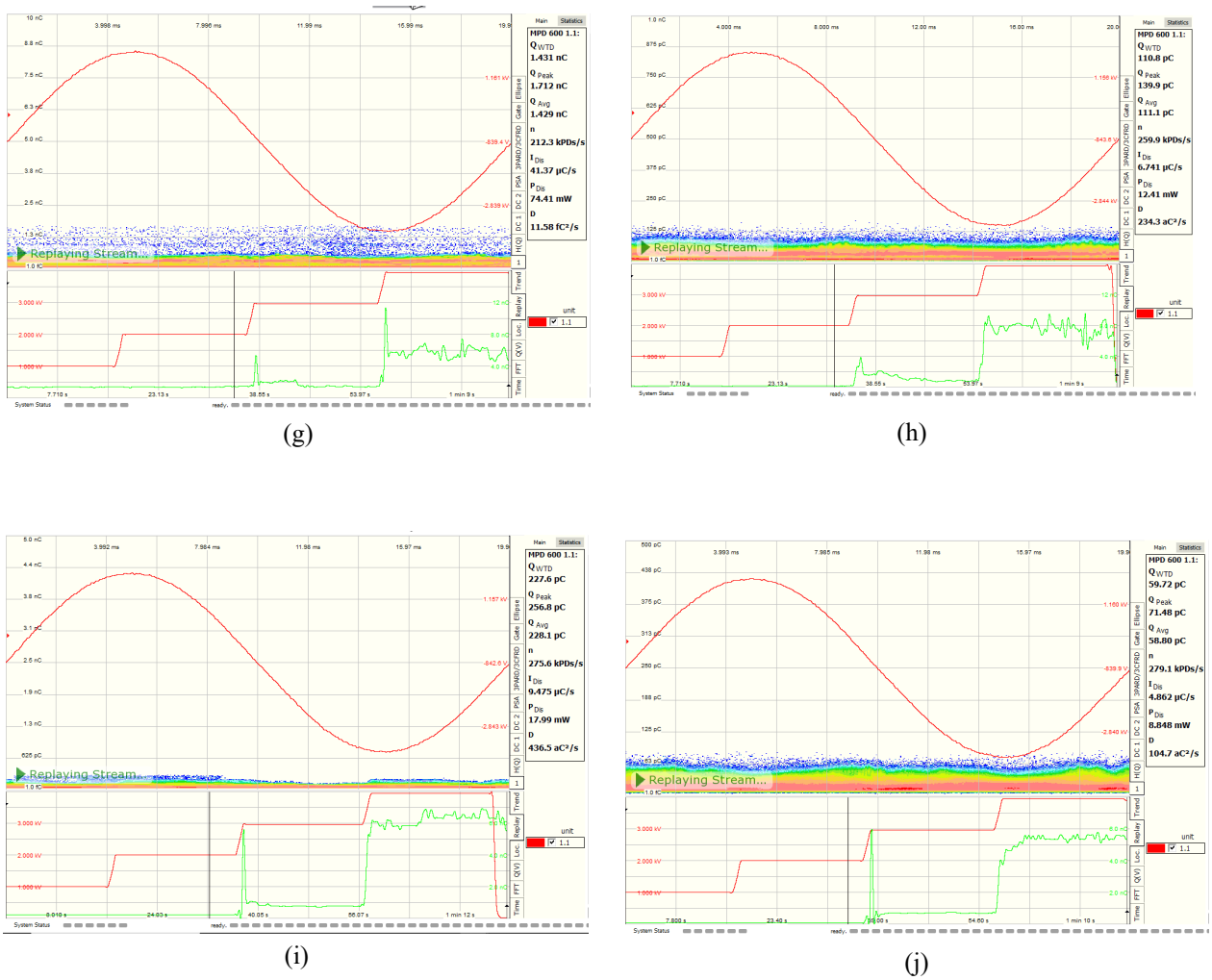

(g) (h)

(i) (j)

Fig 5. PRPD pattern for 2 kV (a) 0.2 MHz, (b) 0.5 MHz, (c) 2 MHz, (d) 6 MHz (e) 10 MHz (f) 12 MHz, (g) 14 MHz, (h) 16 MHz, (i) 18 MHz and (j) 20 MHz.

Table 5 represents a parameter of the PRPD pattern analysis using different frequency bandwidth at 3 kV injection voltage.

Table 5. PRPD parameter at 3 kV

F_{centre} (MHz)	Q IEC/Q WTD (nC)	Q PEAK (nC)	Q AVG (nC)	n (kPDs/s)	PDis (mW)	DF
0.20	9.929	20.31	10.22	61.80	175.0	6.545
0.50	3.916	6.692	3.411	309.9	188.7	4.266
2.00	3.553	6.692	3.441	311.2	191.8	4.266
6.00	0.5316	1.672	0.798	297.3	8.621	2.529
10.00	0.0643	0.0890	0.0615	298.0	3.968	2.682
12.00	0.4399	0.8221	0.4428	285.7	63.40	38.97
14.00	1.411	1.759	1.349	280.2	197.1	114.1
16.00	0.7624	1.128	0.7573	275.9	57.86	46.1
18.00	0.7895	0.9227	0.761	296.2	258.2	198.8
20.00	0.6732	0.8559	0.6814	297.2	240.2	213.6

Fig. 6 (a), (b), (c), (d), (e), (f), (g), (h), (i) and (j) shows the PRPD pattern which clearly shows micro void discharge. Micro void discharge refers to internal discharges that occur mostly in small spaces within the ground wall that act as insulation. The PRPD signature for micro void discharge is shown in Fig. 6 where the micro void discharge exhibits symmetry behavior in the half cycles of the applied sinusoidal voltage with PD activity dominating in the negative half cycle.

The lowest voltage in an insulating system at which PD begins to happen is known as the PDIV. It is the voltage threshold at which PD activity starts and the insulating material starts to degrade. Here, the discharge starts at 3 kV which is the voltage at which PD activity starts. This voltage point is where the insulating material begins to deteriorate, and PD first appears, signaling the start of a potentially harmful process.

Table 6 shows a comprehensive set of parameters derived from PRPD pattern analysis performed at an

injection voltage of 4 kV over various frequency bandwidths. This table provides an overview of PD characteristics that were obtained from the analysis.

Table 6. PRPD parameter at 4 kV

F_{centre} (MHz)	Q_{IEC}/Q WTD (nC)	Q_{PEAK} (nC)	Q_{AVG} (nC)	n (kPDs/s)	PDis (mW)	DF
0.20	24.78	46.03	25.69	63.86	565.2	6.545
0.50	17.71	46.09	19.66	357.2	721.3	4.266
2.00	3.563	8.939	4.309	237.2	57.94	4.266
6.00	3.313	7.491	3.797	293.9	51.66	2.529
10.00	0.2407	0.5562	0.2745	296.1	30.34	2.682
12.00	3.414	4.811	3.087	295.5	490.6	38.97
14.00	4.620	8.916	4.685	295.3	1615	114.1
16.00	7.207	12.03	7.272	299.3	630.7	46.1
18.00	6.359	7.750	6.410	294.8	2978	198.8
20.00	5.386	7.229	5.362	295.7	2520	213.6

Fig. 7 shows visual representations of the PRPD patterns indicating the presence of a micro void discharge where the pattern is symmetrical. The discharge starts at 4 kV which is the PDIV at which PD activity starts. This indicates partial discharge begins to increase as the voltage increases.

Fig. 8 shows frequency against Q_{IEC} where Q_{IEC} is known as is an apparent charge that is measured in accordance with the IEC standard and is stated in pC or nC. An apparent charge cannot be measured directly and is not equal to the quantity of charge locally involved at the discharge point. Fig. 8 also shows the relationship frequency with Q_{IEC} for different voltage. For instance, at 1 kV, the maximum PD charge occurred at the frequency is 0.2 MHz which is 1.952 nC while the minimum charge occurred at 20 MHz which is 65.06 pC.

Similarly, at 2 kV and 3 kV, the trend persists, indicating that higher frequencies correspond to lower PD charge. For 2kV, it shows the maximum PD charge occurred when the frequency is 14 MHz which is 1.431 nC and the minimum charge of PD occurred when the frequency is 20 MHz which is 59.72 pC. Notably, for 3 kV, PD charge is observed at 0.2 MHz which is 9.929 nC while the minimum occurred when the frequency is 20 MHz which is 673.2 pC.

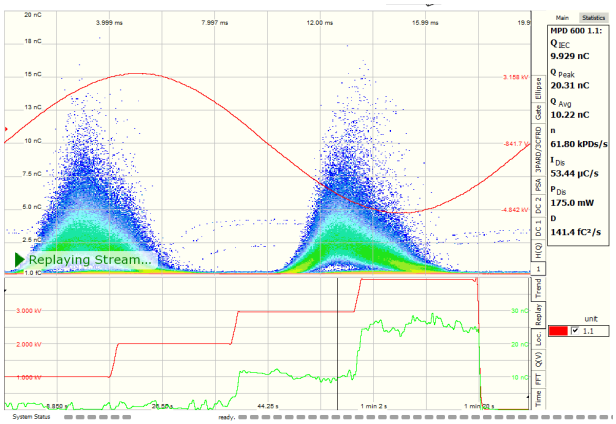

(a)

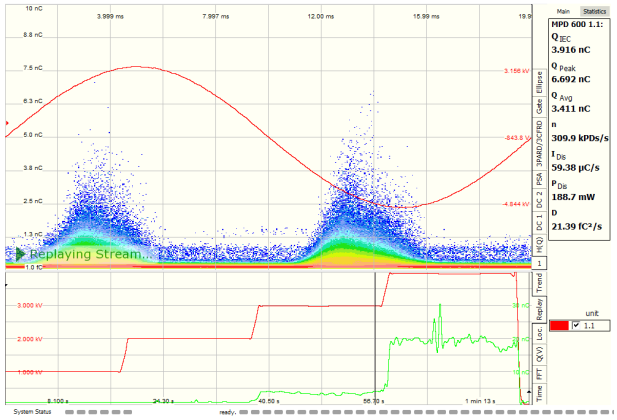

(b)

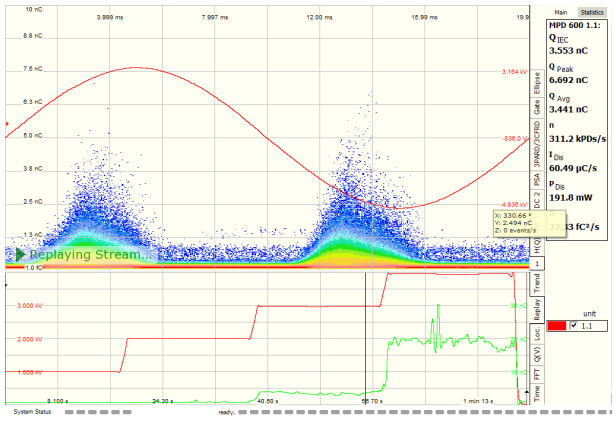

(c)

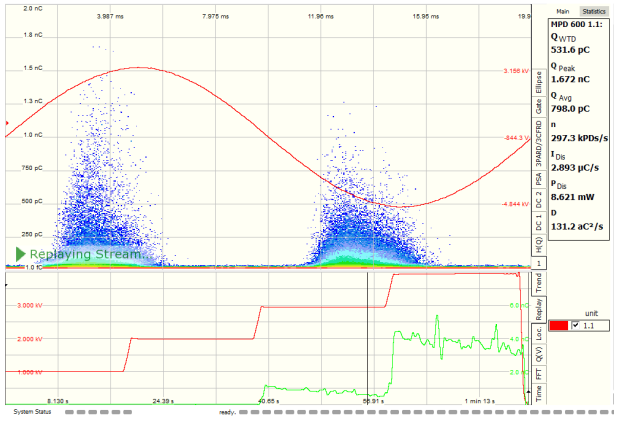

(d)

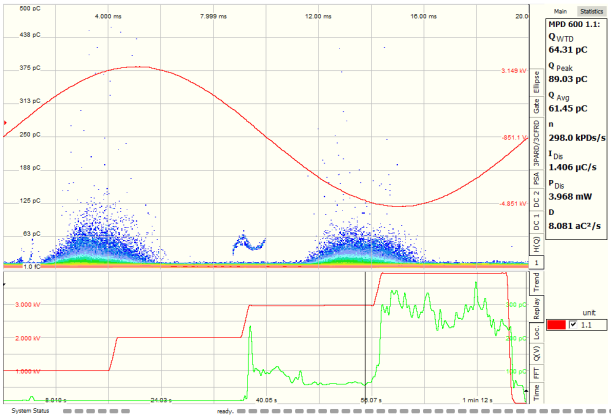

(e)

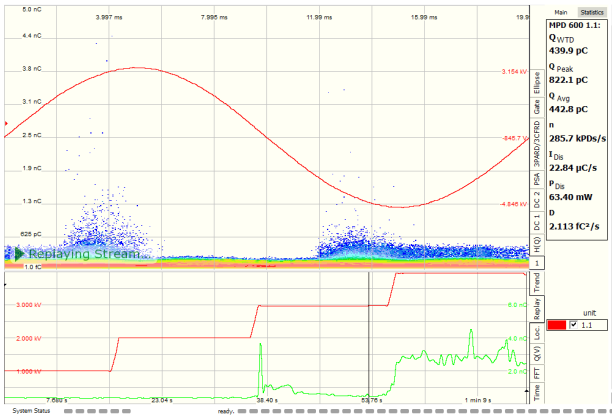

(f)

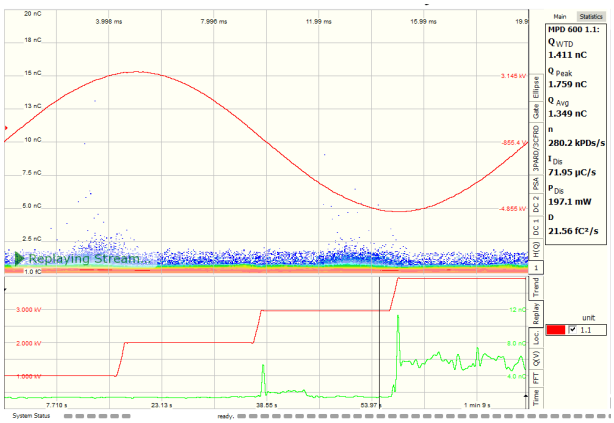

(g)

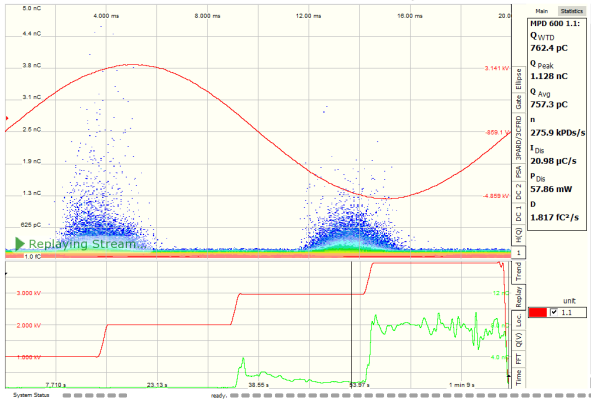

(h)

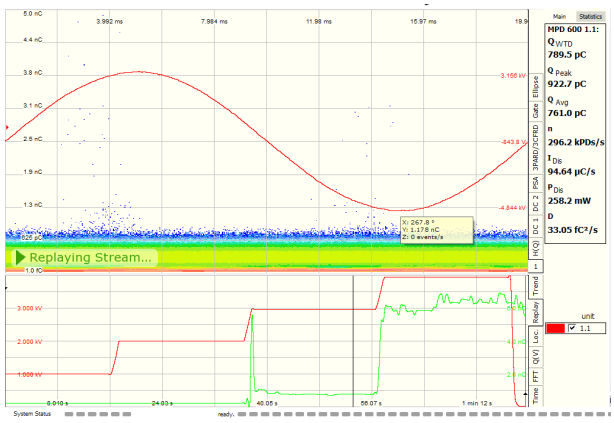

(i)

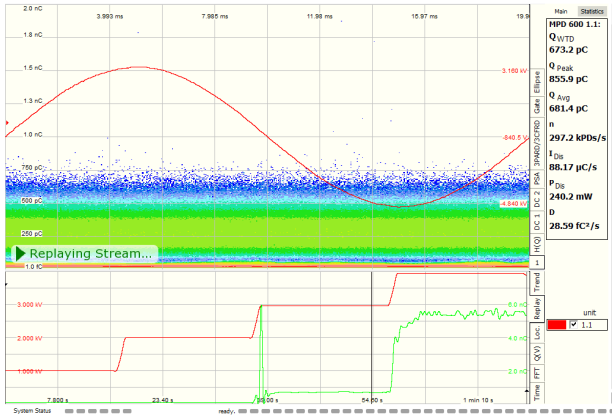

(j)

Fig 6. PRPD pattern for 3 kV (a) 0.2 MHz, (b) 0.5 MHz, (c) 2 MHz, (d) 6 MHz (e) 10 MHz (f) 12 MHz, (g) 14 MHz, (h) 16 MHz, (i) 18 MHz and (j) 20 MHz.

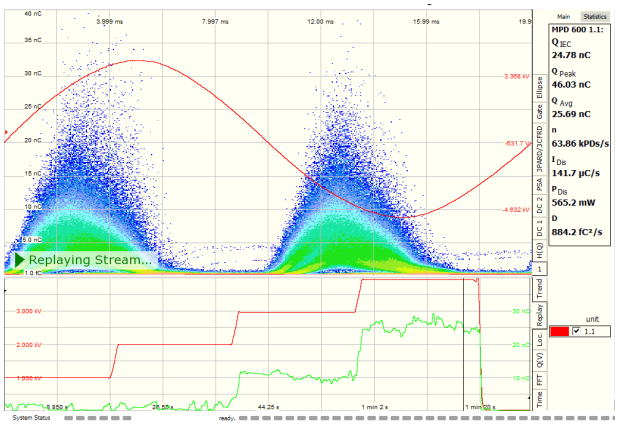
MPD 600 1.1:
Q IEC
24.78 nC
Q Peak
46.03 nC
Q Avg
25.69 nC
n
63.86 kPDs/s
I Dis
141.7 µC/s
P Dis
565.2 mW
D
884.2 fC²/s
Replaying Stream...

(a)

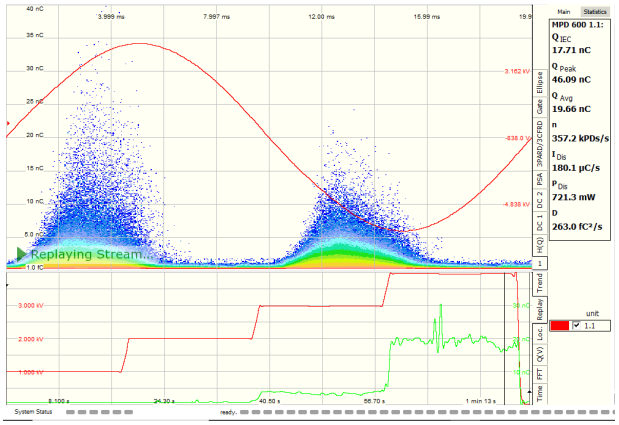
MPD 600 1.1:
Q IEC
17.71 nC
Q Peak
46.09 nC
Q Avg
19.66 nC
n
357.2 kPDs/s
I Dis
180.1 µC/s
P Dis
721.3 mW
D
263.0 fC²/s
Replaying Stream...

(b)

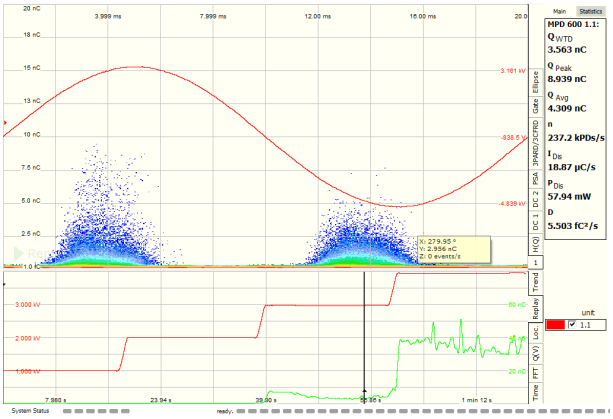
MPD 600 1.1:
Q WTD
3.563 nC
Q Peak
8.939 nC
Q Avg
4.309 nC
n
237.2 kPDs/s
I Dis
18.87 µC/s
P Dis
57.94 mW
D
5.503 fC²/s

(c)

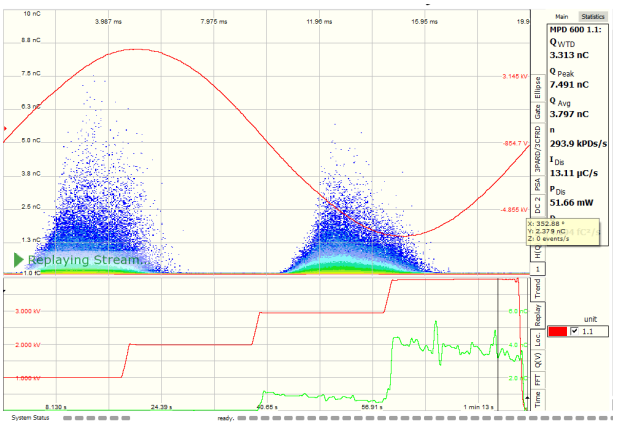
MPD 600 1.1:
Q WTD
3.313 nC
Q Peak
7.491 nC
Q Avg
3.797 nC
n
293.9 kPDs/s
I Dis
13.11 µC/s
P Dis
51.66 mW
Replaying Stream...

(d)

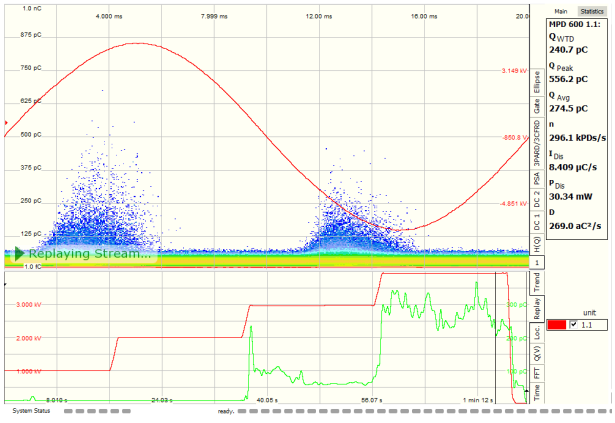
MPD 600 1.1:
Q WTD
240.7 pC
Q Peak
556.2 pC
Q Avg
274.5 pC
n
296.1 kPDs/s
I Dis
8.409 µC/s
P Dis
30.34 mW
D
269.0 aC²/s
Replaying Stream...

(e)

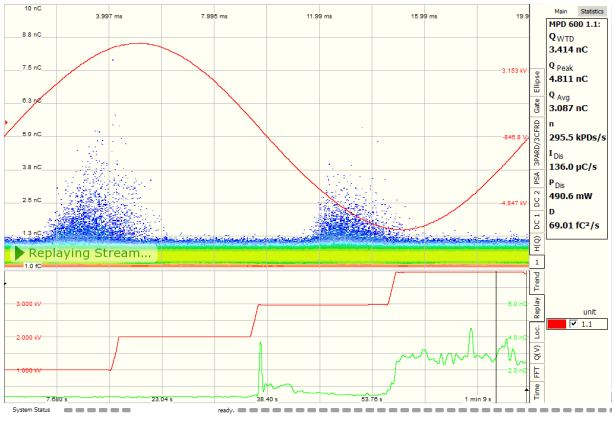
MPD 600 1.1:
Q WTD
3.414 nC
Q Peak
4.811 nC
Q Avg
3.087 nC
n
295.5 kPDs/s
I Dis
136.0 µC/s
P Dis
490.6 mW
D
69.01 fC²/s
Replaying Stream...

(f)

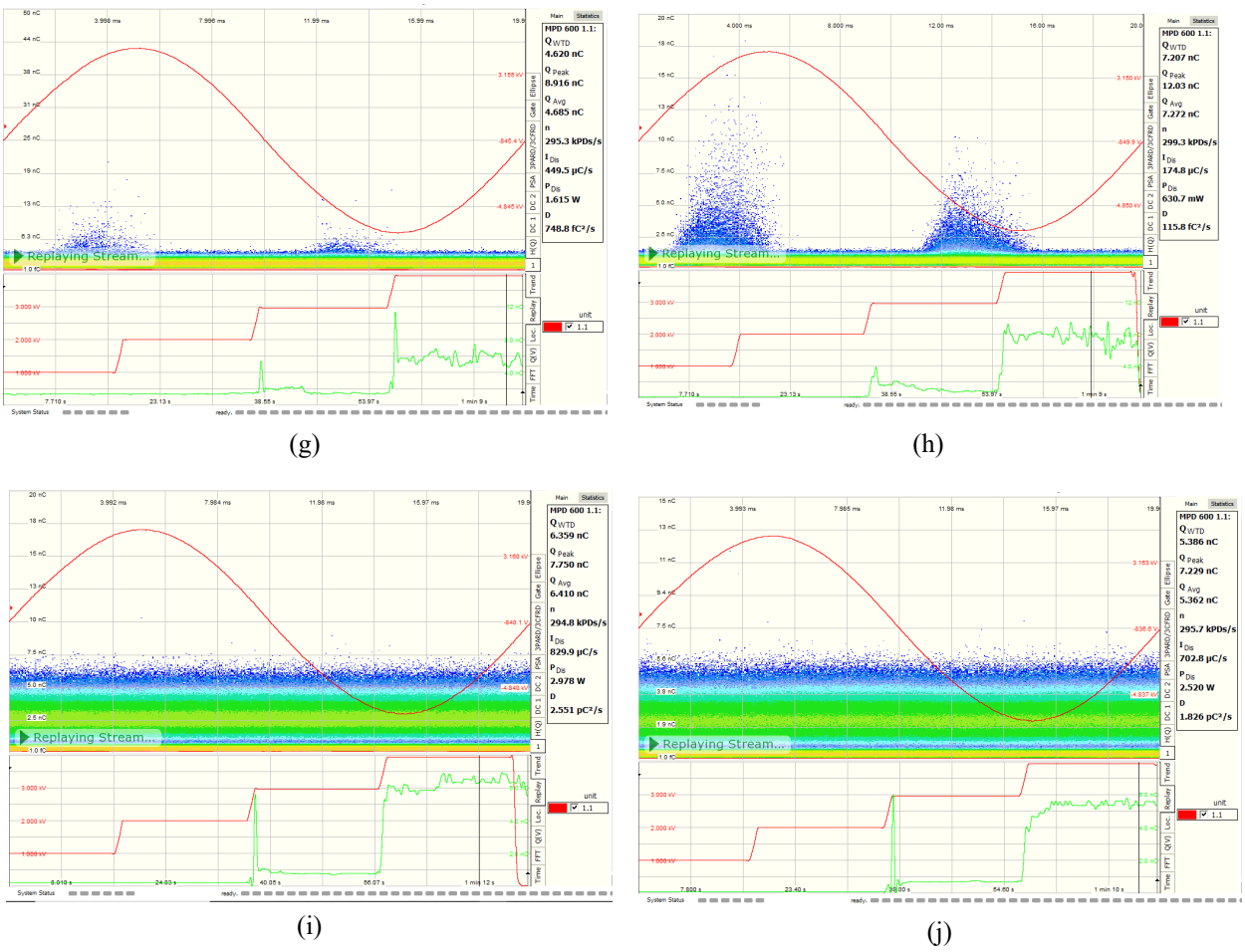

Fig 7. PRPD pattern for 4 kV (a) 0.2 MHz, (b) 0.5 MHz, (c) 2 MHz, (d) 6 MHz (e) 10 MHz (f) 12 MHz, (g) 14 MHz, (h) 16 MHz, (i) 18 MHz and (j) 20 MHz.

Fig. 8 presents frequency against Q_{IEC} where it shows the maximum charge of PD occurred when the frequency is 0.2 MHz which is 24.78 nC and the minimum charge of PD occurred when the frequency is 10 MHz which is 240.7 pC. Thus, the highest Q_{IEC} is at 4 kV while the lowest Q_{IEC} is at 1 kV. This is due to the micro void discharge that is present in winding.

The maximum absolute discharge of every PD event seen during the evaluation interval is represented by Q_{PEAK}, which is its PD magnitude. Fig. 9 shows frequency against Q_{PEAK} for 1 kV where the PD magnitude maximum is observed at Q_{PEAK} of 0.2 MHz which is 2.609 nC. Furthermore, the lowest PD magnitude occurred during frequency of 20 MHz which is 76.85 pC. For instance, at 2 kV, the PD magnitude maximum is observed at Q_{PEAK} of 0.2 MHz which is 3.865 nC. While the lowest PD magnitude occurred during frequency of 20 MHz which is 71.48 pC.

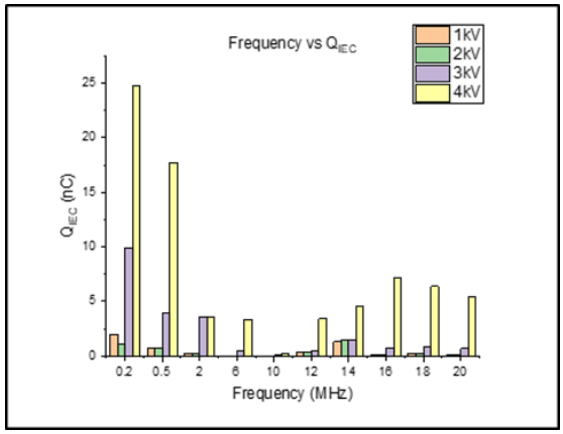

Fig 8. Frequency vs Q_{IEC}

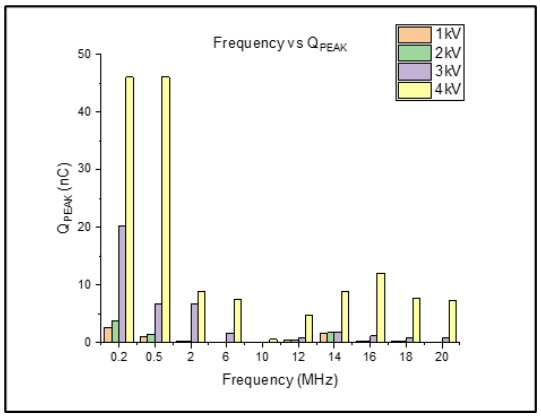

Fig 9. Frequency vs Q_{PEAK}

Fig. 9 shows the PD magnitude maximum is observed at Q_{PEAK} of 0.2 MHz which is 20.31 nC while the lowest PD magnitude occurred during frequency of 20 MHz which is 855.9 pC at 3 kV. The PD magnitude maximum for 4 kV is observed at Q_{PEAK} of 0.2 MHz which is 46.03 nC can be classified as the highest PD magnitude compared than other. However, the lowest PD magnitude occurred during frequency of 10 MHz which is 556.2 pC. Thus, the relationship between frequency and Q_{PEAK}, shows that as frequency increases, the Q_{PEAK} will decrease. This is because there is an increase in micro void discharge at 4 kV although at 3 kV, the micro void discharge starts happening. This indicates that increasing in voltage might increase the PD activity.

According to Fig. 10, the trend of the relationship between frequency and Q_{AVG} shows that as frequency increases, the Q_{AVG} will decrease. This can conclude that Q_{IEC}, Q_{PEAK}, and Q_{AVG} display a similar trend which means that the average charge which is the charge at which PD begin also shows a reduction with increasing frequency. This is due to lower average charge at higher frequencies which may indicate a reduction in the energy released by the individual PD occurrences. This could be a sign of less severe insulation problems, smaller voids, or a different kind of discharge event at higher frequencies.

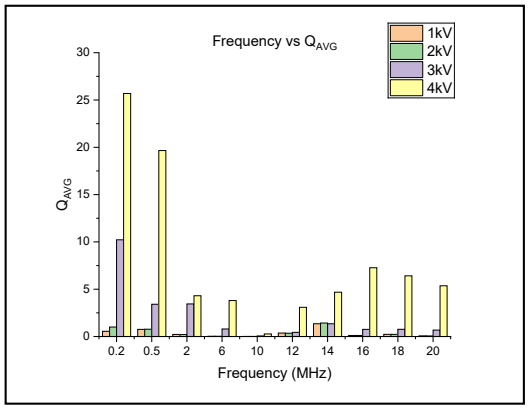

Fig 10. Frequency vs Q_{AVG}

Fig. 11 presents frequency against n (kPDs/s) where n (kPDs/s) is known as PD pulse repetition rate. This is the ratio of the total number of PD recorded in the interval time chosen to the length of this time interval. The highest n (kPDs/s) during the frequency of 20 MHz which is 280.5 kPDs/s for 1 kV while the lowest is 52.77 kPDs/s at 0.2 MHz. Furthermore, at 2 kV, the highest n (kPDs/s) during the frequency of 20 MHz which is 279.1 kPDs/s. However, the lowest occurred during 0.2 MHz which is 58.00 kPDs/s.

Fig. 11 presents the relationship between frequency against n (kPDs/s) for 3 kV where the lowest n (kPDs/s) during the frequency of 0.2 MHz which is 61.80 kPDs/s. The relationship between frequency and n (kPDs/s) for 4 kV is graphically depicted. It shows that 0.2 MHz occurs the lowest PD pulse repetition rate which is 63.86 kPDs/s. Then, the PD pulse repetition rate shows a noticeable increasing trend at 0.5 MHz which is 357.2 kPDs/s.

The most important finding is the abrupt increase in the pulse repetition rate from 0.2 MHz to 0.5 MHz which was followed by a subsequent stabilization of the pulse rate. This is due to higher frequencies can reduce the availability of energy to initiate and sustain PD. This may slow down the overall PD activity and contribute to a stable pulse repetition rate. The graph shows a stable PD pulse repetition rate even as the frequency increases at 6 MHz and above. This indicates the stable PD pulse repetition rate despite increase in frequency due to the lower PD activity.

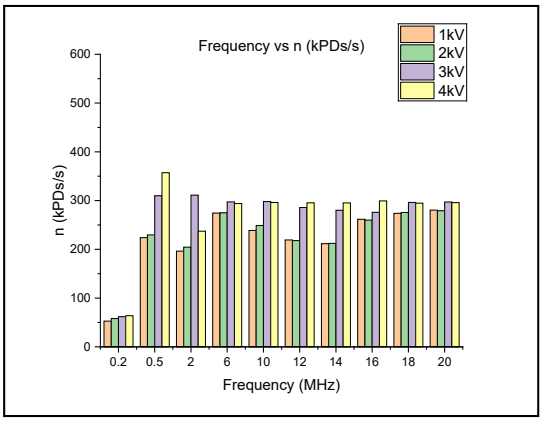

Fig 11. Frequency vs n (kPDs/s)

Fig. 12 shows frequency against PDis for 3 kV where the highest PDis occurs during 18 MHz which is 258.2 mW. This is due to the high PD activity at the frequency 18 MHz. The minimum PDis occur indicates lowest PD activity at frequency of 10 MHz which is 3.968 mW. For 4 kV, the highest PDis happens at 18 MHz and reaches 2978 mW whilst the lowest occurred at 10 MHz which is 30.34 mW. Thus, the highest PDis is at 4 kV compared to the other. One of the most

important parameters is the average discharge power which means larger values indicate that there is more PD activity in the system. In addition, the average discharge power may tend to increase when frequency of PD occurs increase.

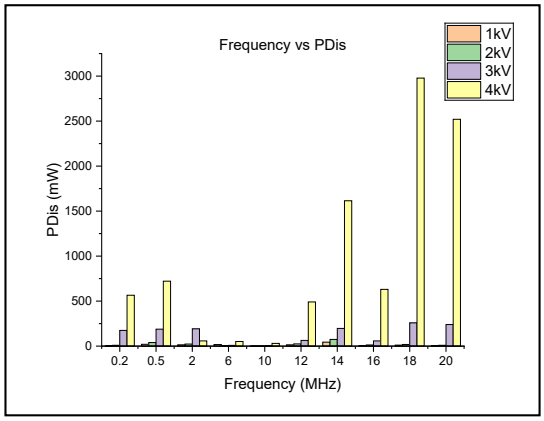

Fig 12. Frequency vs PDis

In summary, partial discharge in rotating machine typically occur in frequency bandwidth of 200 kHz to 300 kHz as specified by standard IEC 60270. This is because the higher frequency signal can propagate through winding and be detected by CC sensor [20]. Furthermore, higher frequency detects PD response more efficiently because the PD responds in the winding insulation produce rapidly rising and high frequency electrical pulses.

4 Conclusion

In conclusion, the study demonstrates the effectiveness of coupling capacitors (CC) for detecting partial discharge (PD) in rotating machines, particularly in the frequency bandwidth of 200-300 kHz as specified by IEC 60270 standards. The research found that PD activity begins at 3 kV (inception voltage) and increases significantly at 4 kV, showing a clear correlation between applied voltage and PD intensity. The analysis revealed that higher frequencies allow better signal propagation through windings and more efficient PD detection due to the rapid rising electrical pulses. The study's findings have important practical implications for industrial maintenance, as they help establish more reliable methods for early detection of insulation problems in rotating machines. This enables better predictive maintenance strategies, potentially reducing operational downtime and preventing catastrophic failures. The research also validates the use of CC sensors for PD monitoring and provides a comprehensive framework for PD measurement and analysis across different frequencies and voltages, contributing to improved diagnostic capabilities in industrial settings. These advancements in PD detection methodology can lead to extended equipment lifespan, enhanced operational safety, and more cost-effective maintenance planning in industrial applications.

Conflict of Interest

The authors declare no conflict of interest.

Author Contributions

Ahmad Syukri Abd Rahman solely conceived and conducted the study. The author prepared the manuscript completely and all authors agreed to be accountable for the content of the work.

Funding

This research was funded by a grant from Ministry of Higher Education of Malaysia (MTUN SEPADAN 2020 (BATCH 2023) and MHH Condition Monitoring Sdn. Bhd.

Informed Consent Statement

Not applicable.

Acknowledgment

The authors would like to express their gratitude to Mohamad Nur Khairul Hafizi Rohani, Afifah Shuhada Rosmi, Ayob Nazmy Nanyan, Nur Dini Athirah Gazata Aiman Ismail Mohamed Jamil, Mohd Helmy Halim Abdul Majid and Normiza Masturina Samsuddin for their valuable assistance and support throughout this study. This work was supported in part by a grant from Ministry of Higher Education of Malaysia (MTUN SEPADAN 2020 (BATCH 2023) and MHH Condition Monitoring Sdn. Bhd.

References

[1] G. C. Stone, H. G. Sedding, C. Chan, and C. Wendel, "Comparison of Low Frequency and High Frequency PD Measurements on Rotating Machine Stator Windings," 2018 IEEE Electr. Insul. Conf. EIC 2018, no. June, pp. 349-352, 2018, doi: 10.1109/EIC.2018.8481128.

[2] F. Oettl, C. Engelen, and C. Staubach, "Localization of PD-events in HV-Windings of Rotating Machines," Diagnostika 2022 - 2022 Int. Conf. Diagnostics Electr. Eng. Proc., no. Figure 2, pp. 1-4, 2022, doi: 10.1109/Diagnostika55131.2022.9905130.

[3] A. Z. Bin Abdullah et al., "Wavelet based de-noising for on-site partial discharge measurement signal," Indones. J. Electr. Eng. Comput. Sci., vol. 16, no. 1, pp. 259-266, 2019, doi: 10.11591/ijeecs.v16.i1.pp259-266.

[4] H. Chai, B. T. Phung, and S. Mitchell, "Application of UHF sensors in power system equipment for partial discharge detection: A review," Sensors (Switzerland), vol. 19, no. 5, 2019, doi: 10.3390/s19051029.

[5] C. L. Wooi, Z. Abul-Malek, M. N. K. Hafizi Rohani, A. M. Bin Yusof, S. N. M. Arshad, and A.

I. Elgayar, "Comparison of lightning return stroke channel-base current models with measured lightning current," Bull. Electr. Eng. Informatics, vol. 8, no. 4, pp. 1478-1488, 2019, doi: 10.11591/eei.v8i4.1613.

[6] C. C. Yii, M. N. K. H. Rohani, M. Isa, S. I. S. Hassan, B. Ismail, and N. Hussin, "Multi-end partial discharge location algorithm based on trimmed mean data filtering technique for MV underground cable," 2015 IEEE Student Conf. Res. Dev. SCOReD 2015, pp. 345-350, 2015, doi: 10.1109/SCORED.2015.7449353.

[7] Y. Yamanaka, T. Umemoto, R. Ikeda, N. Okajima, T. Sakurai, and T. Okamoto, "Deterioration of Corona Armor Tape by Partial Discharge and its Lifetime Evaluation for Form-wound Rotating Machine," 2023 IEEE Electr. Insul. Conf. EIC 2023, pp. 1-4, 2023, doi: 10.1109/EIC55835.2023.10177341.

[8] S. H. K. Hamadi et al., "Modelling of partial discharge signal and noise interference using labview," IEEE Student Conf. Res. Dev. Inspiring Technol. Humanit. SCOReD 2017 - Proc., vol. 2018-Janua, pp. 451-455, 2017, doi: 10.1109/SCORED.2017.8305441.

[9] C. P. Malliou, A. Karlis, and M. G. Danikas, "Electrical machine insulation: Partial discharges, consequences and diagnostic technique," Proc. 2017 IEEE 11th Int. Symp. Diagnostics Electr. Mach. Power Electron. Drives, SDEMPED 2017, vol. 2017-Janua, pp. 468-474, 2017, doi: 10.1109/DEMPED.2017.8062396.

[10] M. Chiampi, G. Crotti, Y. Hu, and A. Sardi, "Calibration of partial discharge measuring systems by a reference impulse charge generator," 16th IMEKO TC4 Int. Symp., pp. 155-160, 2008.

[11] C. Zachariades, R. Shuttleworth, R. Giussani, and R. Mackinlay, "Optimization of a high-frequency current transformer sensor for partial discharge detection using finite-element analysis," IEEE Sens. J., vol. 16, no. 20, pp. 7526-7533, 2016, doi: 10.1109/JSEN.2016.2600272.

[12] S. Chaudhuri, S. Ghosh, D. Dey, S. Munshi, B. Chatterjee, and S. Dalai, "Denoising of partial discharge signal using a hybrid framework of total variation denoising-autoencoder," Meas. J. Int. Meas. Confed., vol. 223, no. September, p. 113674, 2023, doi: 10.1016/j.measurement.2023.113674.

[13] H. M. B. Sibanyoni, J. J. Walker, and J. S. Djeumen, "Evaluation of the behaviour of HFCTs for corona measurement under HVDC application," 2020 Int. SAUPEC/RobMech/PRASA Conf. SAUPEC/RobMech/PRASA 2020, pp. 1-3, 2020, doi: 10.1109/SAUPEC/RobMech/PRASA48453.2020.9041012.

[14] M. A. Kashiha, D. Z. Tootaghaj, and D. Djamshidi, "Partial discharge source classification and denoising in rotating machines using discrete wavelet transform and directional coupling capacitors," Transm. Distrib. Conf. Expo. Asia Pacific, T D Asia 2009, pp. 1-4, 2009, doi: 10.1109/TD-ASIA.2009.5356903.

[15] S. Mohammad Hassan Hosseini and S. Mahdi Mazlomi, "Diagnosing and Online Partial Discharge Location with Using Coupling Capacitor in Induction Motors," GMSARN Int. J., vol. 17, pp. 319-328, 2023.

[16] M. Fritsch and M. Wolter, "High-Frequency Current Transformer Design and Construction Guide," IEEE Trans. Instrum. Meas., vol. 71, pp. 1-9, 2022, doi: 10.1109/TIM.2022.3177189.

[17] Suwarno, "Partial discharge in high voltage insulating materials," Int. J. Electr. Eng. Informatics, vol. 8, no. 1, pp. 147-163, 2016, doi: 10.15676/ijeei.2016.8.1.11.

[18] Z. Faizol et al., "Detection Method of Partial Discharge on Transformer and Gas-Insulated Switchgear: A Review," Appl. Sci., vol. 13, no. 17, 2023, doi: 10.3390/app13179605.

[19] M. M. Yaacob et al., "Review on partial discharge detection techniques related to high voltage power equipment using different sensors," Photonic Sensors, vol. 4, no. 4, pp. 325-337, 2014, doi: 10.1007/s13320-014-0146-7.

[20] M. M. Yaacob, M. A. Alsaedi, J. R. Rashed, A. M. Dakhil, and S. F. Atyah, "Review on partial discharge detection techniques related to high voltage power equipment using different sensors," Photonic Sensors, vol. 4, no. 4, pp. 325-337, 2014, doi: 10.1007/s13320-014-0146-7.

Biographies

Ahmad Syukri Abd Rahman received a Bachelor of Information Technology (Graphics & Multimedia) (Hons) programme at Universiti Tenaga Nasional, Kajang Selangor, Malaysia and was graduated in 2016. He is currently pursuing his Msc in Electrical Engineering at Universiti Malaysia Perlis. The author's current job as Assistant Operation Manager at MHH Condition Monitoring Sdn. Bhd, Selangor, Malaysia. His research interests include analysis of PD measurement in rotating machine.

Mohamad Nur Khairul Hafizi Rohani was born in Johor, Malaysia, in 1989. He received the Diploma degree in computer engineering, the B.E. degree (Hons.) in industrial electronic engineering, and the Ph.D. degree in electrical system engineering from Universiti Malaysia Perlis, Malaysia, in 2010, 2013, and 2017, respectively. Currently, he is a Associate Professor in Faculty of Electrical Engineering & Technology, Universiti Malaysia Perlis. He is also a Research Fellow of the High Voltage Centre of Excellence for Renewable Energy (CERE) and a member of the High Voltage and Transient Insulation Health Research Group. His research interests include partial discharge detection and measurement on solid and liquid insulation, signal and image processing, and partial discharge sensor development for high voltage equipment applications.

Nur Dini Athirah Gazata was born in Kangar, Perlis. She received a Bachelor of Electrical Engineering (Honours) at Universiti Malaysia Perlis, Perlis, Malaysia and was graduated in 2023. She is currently studying her Msc in Electrical Engineering at Universiti Malaysia Perlis. Her research interests include analysis PD in high voltage rotating machine.

Afifah Shuhada Rosmi was born in Johor, Malaysia. She was an accomplished researcher in electrical engineering, specializing in piezoelectric energy harvesting and partial discharge monitoring. She earned her PhD in Electrical Engineering Systems in 2018 and her bachelor's degree in Electrical System Engineering in 2013, both from Universiti Malaysia Perlis (UniMAP). With a passion for advancing sustainable energy solutions, Dr. Afifah has made significant contributions to her field through innovative research and practical applications.

Ayob Nazmy Nanyan was born in Langkawi, Malaysia. He received his Ph.D. in Electrical Systems Engineering from Universiti Malaysia Perlis (UniMAP) in 2021. He holds a Master of Science (M.Sc.) in Electrical Power Engineering from UniMAP, which he obtained in 2015, and a Bachelor of Engineering (B.Eng. Hons.) in Electrical Systems Engineering from the same institution in 2007. From 2007 to 2015, Dr. Ayob gained extensive professional experience as an Electrical Engineer, contributing to power plant and hospital infrastructure projects. His expertise lies in electrical systems, power engineering, and infrastructure development.

Aiman Ismail Mohamed Jamil received a Master of Science in Electrical Power Engineering at Universiti Malaysia Perlis, Perlis, Malaysia and was graduated in 2023. He is currently pursuing his PhD in Electrical Engineering at Universiti Malaysia Perlis. His research interests include in the analysis of PRPD pattern identification in rotating machine using DLMs.

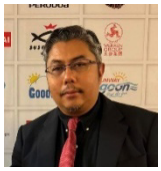

Mohd Helmy Halim Abdul Majid a graduate with a Bachelor's degree in Electrical and Electronics Engineering from Northumbria University, U.K., is the Managing Director of Heliz & Rasraaf Sdn Bhd. Renowned for his engineering and management expertise, he focuses on total predictive maintenance, encompassing business development, marketing, project management, and field technical support in the global market. Heliz & Rasraaf Sdn Bhd, an independent engineering consultancy firm, provides predictive maintenance services and turnkey solutions across various industries.

Normiza Masturina Samsuddin a graduate with a Bachelor's degree in Electrical Engineering from Universiti Teknologi MARA (UiTM), also holds a Foundation degree in Engineering from the same institution. She is currently a Research Officer at MHH Condition Monitoring Sdn Bhd. With a focus on engineering excellence, she contributes to the development and implementation of advanced condition monitoring solutions. Her role involves enhancing equipment reliability and optimizing maintenance strategies, supporting industries in achieving operational efficiency and cost-effectiveness.